THE JOURNAL OF PHYSICAL CHEMISTRY Letters

Letter

pubs.acs.org/JPCL

Probing the Structure of Salt Water under Confinement with First-Principles Molecular Dynamics and Theoretical X-ray Absorption Spectroscopy

Heather J. Kulik,[†] Eric Schwegler,[‡] and Giulia Galli*[,¶]

[†]Department of Chemistry, Stanford University, 333 Campus Drive, Mudd Building Room 121, Stanford, California 94305, United States

[‡]Physical and Life Sciences Directorate, Lawrence Livermore National Laboratory, 7000 East Avenue, PO Box 808, L-415, Livermore, California 94550, United States

[¶]Departments of Chemistry and Physics, University of California—Davis, One Shields Avenue, Davis, California 95618, United States

ABSTRACT: We investigated the structure of liquid water around cations (Na^+) and anions (Cl^-) confined inside of a (19,0) carbon nanotube with first-principles molecular dynamics and theoretical X-ray absorption spectroscopy (XAS). We found that the ions preferentially reside near the interface between the nanotube and the liquid. Upon confinement, the XAS signal of water molecules surrounding Na^+ exhibits enhanced pre-edge and reduced post-edge features with respect to that of pure water, at variance with the solvation shell of Na^+ in bulk water. Conversely, the first solvation shell of confined Cl^- has a main-edge intensity comparable to that of bulk solvated Cl^-, likely as a result of a high number of acceptor hydrogen bonds in the first solvation shell. Confined nonsolvating water molecules exhibit bulk-like or water-monomer-like properties, depending on whether they belong to core or interfacial layers, respectively.

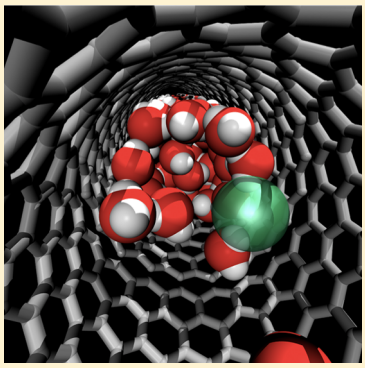

SECTION: Liquids; Chemical and Dynamical Processes in Solution

Understanding the complex behavior of water and aqueous solutions in confined environments,[1] such as in cavities and channels, is key for a variety of fields from biology[2−5] to materials science.[6−8] However, many fundamental properties of confined water have yet to be fully understood.[9] For example, both theory[10−13] and experiments[6,14,15] have indicated that water in carbon nanotube (CNT) channels exhibits anomalous properties, ranging from fast[6] to slow[14] transport.[15] Single-walled CNTs are excellent models of confining media found in complex systems, such as biological membrane pores.

Several experimental techniques, including X-ray diffraction (XRD),[16−18] extended X-ray absorption fine structure (EXAFS) spectroscopy,[19] and neutron diffraction[20,21] have been used to elucidate the coordination number of ions in bulk water. In addition, core-level X-ray absorption spectroscopy (XAS) measurements have provided a detailed view of the nature of ion solvation.[22] In fact, experimental XAS results indicate that the enhancement of pre- and main-edge spectral features of salt solutions with respect to pure liquid water can be ion-specific. Recent neutron diffraction studies of $CaCl_2$ and $MgCl_2$ have also pointed out cation-specific features in solution.[23]

Molecular dynamics (MD) simulations with classical force fields have been used to study the structure of salt solutions in a variety of conditions, including bulk and nanoconfined media. It is now clear that nonpolarizable force fields tend to overestimate the rigidity and coordination number of the solvation shell of most cations and anions.[17,24] Furthermore, as pointed out in a recent review,[25] water models parametrized for bulk water may not be transferable to solid−water interfacial systems. For example, conflicting predictions have been reported on the dynamics of liquid between smooth hydrophobic surfaces when different classical models are used.[26−31] Although computationally expensive, ab initio approaches do not rely on empirical parameters and are thus applicable to a wide range of conditions and systems. In particular, first-principles MD simulations have successfully predicted experimental coordination numbers for Na^+[32] and other ions in bulk liquid solutions. Furthermore, the calculation of X-ray absorption spectra of bulk salt solutions[22,33] using ab initio MD trajectories has recently shown a clear correspondence between the features of the spectrum and local electronic and geometric properties of the liquid, such as ion−water tilt angles and hydrogen-bonding network configurations.

Here, we present the analysis of a first-principles MD simulation of salt water (containing Na^+ and Cl^-) confined inside of a (19,0) single-walled CNT. We find that the ions are preferentially located near the water−nanotube interface, consistent with previous observations for the air−water interface.[34] We used the calculated XAS of select MD snapshots

Received: July 11, 2012
Accepted: September 5, 2012

   dx.doi.org/10.1021/jz300932p | J. Phys. Chem. Lett. 2012, 3, 2653−2658

to uncover the dependence of spectral features on both the orientation of water molecules and the hydrogen-bonding network. We compared the properties of the first solvation shell around Na^+ and Cl^- in confined and liquid-like environments, and we identified differences in the X-ray absorption spectrum of nonsolvating water molecules in a confined environment according to the radial distance from the center of the nanotube.

We adopted the PBE functional and plane wave basis sets,[35] as implemented in the Qbox code,[36] with norm-conserving pseudopotentials (PPs) and a wave function cutoff of 85 Ry. The sodium 2s and 2p electrons were included among the valence states. We used a tetragonal simulation cell ($a = b =$ 21.17 Å, c = 17.06 Å) containing one Na^+ cation and one Cl^- anion as well as 52 water molecules inside of 4 repeats of a primitive unit cell of a (19,0) CNT ($d \approx 1.4$ nm); this corresponds to a 1.0 M concentration for the salt solution with a density of ~1 g/cm^3. The simulation cell used here originates from the simulations reported in ref 10, where numerous classical MD runs of water confined by both graphitic sheets and CNTs were carried out in order to accurately determine the equilibrium density of the confined liquid (as described by the SPC/E water model). The final configuration obtained in the classical simulations of water inside of a (19,0) CNT was used to carry out a 23 ps first-principles MD simulation of pure water at elevated temperature (~400 K). We then removed two of the water molecules from the last configuration of the FPMD run; these molecules were randomly selected from the central water layer and replaced by a sodium and a chloride ion. A 5 ps FPMD simulation was then carried out to equilibrate the newly obtained solution, followed by a 14 ps trajectory, which we analyze below. We note that an elevated temperature was used to avoid overstructuring and slow diffusion of liquid water, which commonly occur when using GGA functionals at ambient temperature and pressure.[37] The results of BOMD simulations of NaCl solvated in bulk water were taken from ref 33.

X-ray absorption spectra corresponding to the oxygen near-K-edge were calculated for the confined NaCl solution with the method implemented in the Quantum-ESPRESSO code[38] using ultrasoft PPs that, in the case of oxygen, require a cutoff of 25 Ry. The XAS were calculated on water molecules selected from 10 equally spaced snapshots of the trajectories generated for the confined salt water system. For the first solvation shell, this corresponds to 37 molecules sampled around the sodium cation and 31 around the chloride anion, which is consistent with sample sizes used in previous studies.[33,39] A total of 80 nonsolvating water molecules were selected across the same 10 snapshots to ensure that a range of radial distances from the center of the tube was properly sampled. Spectral properties of the first solvation shell water molecules around Cl^- in bulk liquid water were obtained using a comparable procedure, sampling 40 water molecules belonging to 10 snapshots used previously for Na^+.[33] In order to mimic the X-ray excitation process that results in the formation of a core hole, the final state of the electronic system was calculated for a snapshot where the PP of one neutral oxygen atom is replaced with a PP representing an oxygen atom with a core hole in its 1s level.[39] The matrix elements between the atomic core level and the excited conduction band were computed using a frozen core approximation.[39−42] The k-point mesh for the XAS calculations was chosen based on previous results[12] to be six k-points evenly spaced along the tube axis. The computed spectrum was aligned with an onset energy of 535 eV associated with the lowest computed transition and broadened by 0.15 eV with a Gaussian line shape (see ref 43 for a detailed discussion of alignment schemes). We note that this approach may yield an approximate and not fully accurate description of the screening of excited states higher than the first one, but such a limitation should not significantly impact our qualitative comparisons of spectral features arising from different water molecules in the liquid.

Both first-principles and classical MD simulations were carried out on confined NaCl solutions in a (19,0) CNT. As illustrated in Figure 1, the comparison of radial atomic density

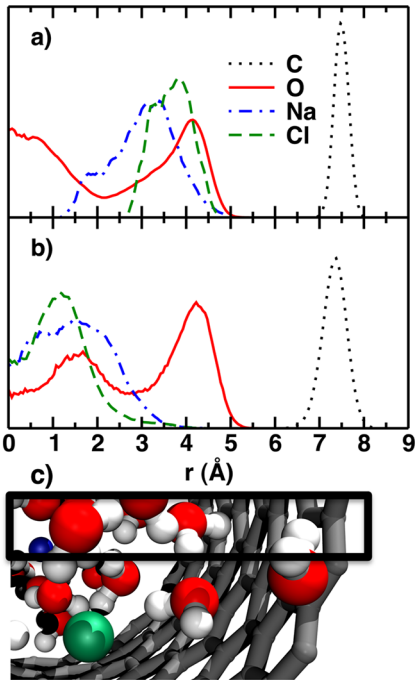

Figure 1. The radial atomic density distributions for oxygen (red solid line), carbon (dotted black), sodium (dotted−dashed blue), and chloride (dashed green) inside of a liquid-filled CNT from (a) first-principles MD and (b) classical MD with a nonpolarizable force field as a function of the distance from the center of the nanotube; the geometrical arrangement is shown in (c).

distributions obtained from first-principles and classical simulations of confined NaCl solutions reveals significant differences. The classical simulations were carried out with nonpolarizable force fields; in those simulations, the Na^+ and Cl^- ions tend to reside near the center of the CNT where they are fully solvated by water molecules. Conversely, in the first-principles simulations, the ion distributions are peaked noticeably closer to the nanotube−water interface, with the chloride ion slightly closer to the surface than sodium. This apparent accumulation of ions near the CNT−water interfacial region is similar to what has been observed in classical simulations of the air−water interface[44,45] and, more recently, of water confined by graphene sheets[46] when ion polarizability is taken into account. There is increasing evidence indicating that interactions between solvated ions and interfaces are strongly influenced by the chaotropic/kosmotropic character of the ions, as well as by the overall hydrophobic/hydrophilic character of the surface.[47,48] In the case of a salt solution in contact with a hydrophobic surface, strongly solvated

kosmotropic ions tend to retain their solvation shell and are repelled by the interface; instead, chaotropic ions, which are more polarizable, can rearrange their electronic distribution to compensate for the penalty associated with losing a water solvation shell as the interface region is approached. The trend shown in Figure 1a is consistent with the view[49,50] of Na^+ and Cl^- being considered as weakly kosmotropic and chaotropic ions, respectively.[51] In addition, the lack of ion accumulation near the interface when using nonpolarizable potentials (Figure 1b) is consistent with previous studies that found that anion concentrations near hydrophobic surface-water interfaces strongly depend on the extent to which ion polarization is taken into account.[44−46,52]

We turn to the discussion of specific orientational effects associated with interfacial water molecules. As shown in the first-principles simulations of ref 10, a specific distribution of O−H tilt angles is found at the interface between water and graphene or water and CNTs (see Figure 2 of ref 10). We have carried out a similar analysis of the O−H bond tilt angle distribution as a function of the distance from the center of the CNT (see Figure 2). For distances 4−5 Å from the center,

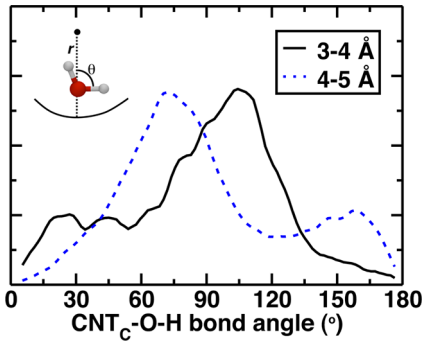

Figure 2. The distribution of O−H bond tilt angles with respect to the center of the nanotube within a radial shell of 3−4 Å (solid black line) and 4−5 Å (blue dashed line) from the center of the nanotube, as depicted in the inset.

there is a prominent peak at 75° that corresponds to O−H bonds that are approximately parallel to the CNT surface and a smaller peak at 165° that corresponds to O−H bonds that are pointing toward the surface. For distances closer to the center of the CNT, in the range of 3−4 Å, the most prominent peak smoothly shifts toward larger angles at 115°, and a smaller peak appears at 20°, which corresponds to O−H bonds that are pointing toward the center of the CNT. We emphasize that the overall O−H bond tilt angle distributions shown in Figure 2 are not sensitive to the presence (or absence) of the salt and are primarily properties of the water−CNT interface. The slight preference for the interfacial water molecules to orient an O−H bond toward the CNT surface provides a favorable surface dipole to which a polarizable anion can align.

We now consider the structural changes that the first hydration shell undergoes when salt solutions are placed under confinement. Comparisons of coordination numbers (Table 1) suggest that the average number of water molecules immediately surrounding Na^+ and Cl^- decreases from bulk to the confined environment and that the maximum of the coordination number distributions also decreases, although definite, quantitative statements would require longer simulations, averaged on several samples. Analysis of the distance from Na^+ or Cl^- to the center of mass of the first solvation shell

Table 1. Comparison of Bulk and Confined Solvation Shell Properties for Na^+ and Cl^-, Including the Coordination Number (determined from Na−O and Cl−H distances, respectively) and the Probability Distribution of the First Solvation Shell Center of Mass to the Relevant Ion ($r_{ion-NN_{COM}}$)

	coordination (#)			$r_{ion-NN_{COM}}$ (Å)	
	avg	range	σ	max	σ
Na^+ bulk	5.2	3−9	0.75	0.35	0.20
Na^+ confined	4.9	3−8	0.94	0.35	0.27
Cl^- bulk	4.9	2−8	0.86	0.45	0.20
Cl^- confined	4.5	3−7	0.71	0.65	0.23

water molecules (Table 1) provides a measure of the asymmetrical distortion around the ions. This measure of distortion indicates whether the ions are partially desolvated as asymmetries in the solvation shell are expected to occur when ions reside at an interface or are placed under confinement. The measure of distortion for Na^+ first solvation shell water molecules is the same in bulk and confined environments, around 0.35 Å. In the bulk, asymmetry of water molecules around Cl^- appears to be larger because the distance of the ion to the first solvation shell center of mass is 0.45 Å. This distortion increases significantly (to 0.65 Å) when Cl^- is solvated in confined water. The reduced rigidity of the Cl^- solvation shell combined with the propensity of the anion to reside near the interface results in an increased distortion of the chloride first solvation shell under confinement, with respect to sodium.

X-ray absorption spectroscopy can provide further valuable insight into how the electronic and geometric structure of water and salt solutions depends on confinement. In particular, theoretical X-ray absorption spectra may be analyzed in terms of features arising from specific ions or from different microenvironments of the water molecules. Following the observation of a distinct inner core of bulk-like and outer shell of water-monomer-like water molecules, we considered the radial dependence of X-ray absorption spectra for water in the (19,0) CNT. Inspection of the radial density distribution of oxygen from the center of the tube outward (Figure 1a) confirms the presence of an inner and outer region, each peaked at around 0 (the center of the tube) and 4 Å, respectively. We also identified a transition region between the inner and outer regions from 1.75 to 2.75 Å consisting of water molecules exchanging between inner and outer regions. As shown in Figure 3, inner-region water molecules exhibit features relatively close to those previously observed in experimental[22] and calculated theoretical bulk liquid water spectra.[33]

The inner region water molecules still exhibit lower post-main-edge intensity and slight enhancement of the pre-edge peak with respect to that of bulk water.[33] Enhancement of pre-edge peak features typically corresponds to an apparent reduction in hydrogen bonding;[33,39] in the confined environment, reduced hydrogen bonding is likely due to a lack of interactions beyond nearest neighbors and to frustration induced by the presence of surfaces. The outer-region water molecules have a very prominent pre-edge peak and enhanced first main-edge peak consistent with water molecules with reduced hydrogen bonding.[39] The rate of decline of post-main-edge intensity is also much larger in the outer region. The

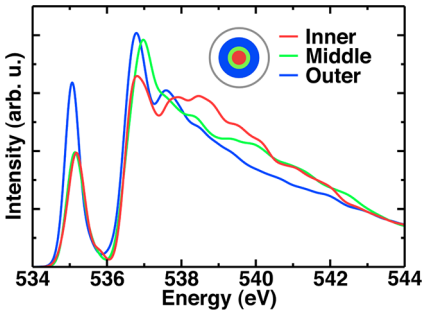

Figure 3. The XAS features of nonsolvating, confined water molecules are compared for three regions, inner (red, 0−1.75 Å), middle (green, 1.75−2.75 Å), and outer (blue, 2.75−5 Å) (see the text).

spectrum associated with the transition region has a decreased pre-edge peak, comparable to that of the inner region, but main-edge and post-main-edge features are more closely related to those of the outer-region spectrum. Because our analysis of the radial atomic density distributions indicates that both Na^+ and Cl^- reside in the outer region, we expect that the features of the XAS of first solvation shell water molecules in the CNT will be distinct from the corresponding ones in bulk solutions.

The averaged spectral features of the solvation shell of Na^+ in confined water (Figure 4) show significant reduction in the

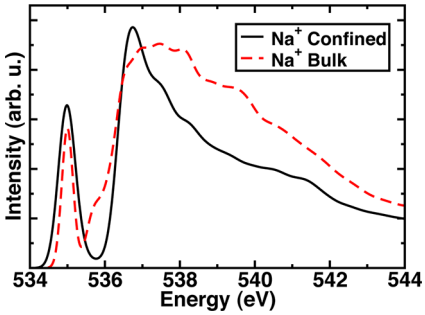

Figure 4. Comparison of XAS for Na^+ first solvation shell molecules in confined (black) and bulk (red, dashed) water.

main-edge and post-main-edge intensity from previous results on bulk water[39] and salt solutions,[33] indicating that water molecules are in a water-monomer-like microenvironment. Both Na^+ and Cl^- preferentially occupy the interfacial shell of water molecules, which is a region characterized by distinct tilt angles and XAS features corresponding to reduced hydrogen bonding. In the case of Na^+, solvating water molecules orient with oxygen atoms toward the cation and hydrogen atoms directed outward, thus forming donating hydrogen bonds with neighboring water molecules. In bulk water, the solvation shell structure around Na^+ enables the formation of accepting hydrogen bonds as well. We previously observed these acceptor hydrogen bonds to be correlated to enhanced main-edge and post-main-edge peaks.[33] Calculation of hydrogen-bonding configurations of the first solvation shell of Na^+ under confinement indicates that the dominant contribution is from water molecules without acceptor bonds (Table 2). We found that water molecules in no-acceptor configurations (0D + 0A and 1D + 0A) are increasing under confinement, while configurations with acceptor hydrogen bonds are decreasing (1D + 1A, 2D + 1A). As mentioned earlier, there is little increase in distortion of the solvation shell from bulk to confinement (see Table 1). This relative inflexibility of the

Table 2. Comparison of the Hydrogen-Bonding Network for the First Solvation Shell around Na^+ and Cl^- in Bulk and Confined Liquid Water Environments[a]

		Na^+		Cl^-	
D	A	bulk	confined	bulk	confined
0	0	**8**	**22**	**9**	**19**
0	1	6	4	**11**	**24**
0	2	0	0	8	10
1	0	**17**	**34**	7	7
1	1	**31**	**16**	30	24
1	2	1	0	**29**	**14**
2	0	11	12	1	1
2	1	**25**	**11**	2	1
2	2	1	0	3	0

[a]The percentage of each combination of donor (D) and acceptor (A) hydrogen bonds formed by first solvation shell water molecules throughout the MD trajectory is reported. The most significant changes from bulk to confinement are highlighted in bold.

solvation shell may cause water molecules to form unfavorable geometries (from a hydrogen bonding point of view) that give rise to narrower XAS features under confinement.

In contrast with Na^+, solvating water molecules around Cl^- orient with one hydrogen atom toward the anion and oxygen atoms directed outward. This orientation leaves the other hydrogen atom available to donate hydrogen bonds, and the oxygen is accessible to form acceptor bonds. In bulk liquid, the XAS of water molecules in the first solvation shell around Cl^- exhibits reduced post-main-edge features corresponding to a smaller number of hydrogen bonds than that in the bulk or within the cation solvation shell.[33] In confinement, however, the spectral features are relatively unchanged (Figure 5), with

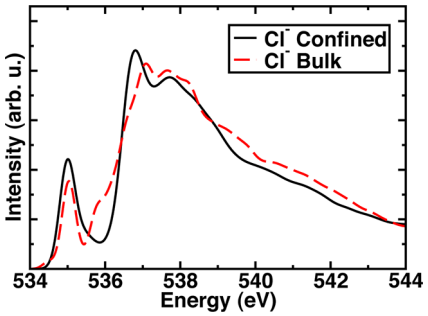

Figure 5. Comparison of XAS for Cl^- first solvation shell molecules in confined (black) and bulk (red, dashed) water.

the post-main-edge peak only slightly decreased and the pre-edge one slightly increased. In examining how the hydrogen bonding of first solvation shell water molecules around Cl^- change from bulk to confinement, we observed an enhancement in some low-hydrogen-bonding (0D + 0A) configurations (Table 2). However, the number of acceptor hydrogen bonds formed over all configurations is relatively stable, with some increasing (0D + 1A, 0D + 2A) ones. The solvation shell of the chloride anion was observed both to be more distorted than that of the cation in the bulk and to become even more distorted under confinement (see Table 1). Analogous to anions at the air−water interface, this change in the chloride ion solvation shell under confinement may be understood in terms of changes in polarization; polarizable anions are stabilized at the interface when they acquire a dipole in the presence of the

dx.doi.org/10.1021/jz300932p | J. Phys. Chem. Lett. 2012, 3, 2653−2658

surface that compensates for a loss of solvation energy and increased electrostatic repulsion.[53] The weaker interactions between chloride and solvating water molecules, with respect to cations, produce nearly equivalent XAS for solvating water molecules in bulk and confinement. This observation is also consistent with previous classical, polarizable force field simulations that suggested that the underlying mechanisms that lead to preference for Cl^- accumulation near a hydrophobic interface are more complicated than simple polarizability arguments and involve an enhancement of water−water interactions.[52]

In summary, we have presented predictions of the structural and electronic properties of salt water confined inside of a CNT. Our first-principles MD and calculated X-ray absorption spectra revealed the presence of two distinct shells of water molecules in the nanotube, an inner "bulk-like" core and an outer interfacial shell resembling the air−water interface. We have shown that both sodium cations and chloride anions preferentially occupy the interfacial region, with chloride ions residing farthest from the center of the nanotube. Confinement has a stronger effect on the relative distortion of the flexible chloride solvation shell than on the more rigid sodium shell. The flexibility around chloride permits first solvation shell water molecules to form roughly the same number of acceptor hydrogen bonds with nearest-neighbor water molecules in the bulk or under confinement, thus giving rise to essentially environment-independent XAS features. The rigidity of the sodium solvation shell, on the other hand, results in a strong decrease in the number of acceptor bonds from bulk to confinement, producing a significantly more water-monomer-like XAS for first solvation shell water molecules in confinement. In general, hydrogen-bonding effects play a much larger role in determining XAS features than subtler, interface-driven differences in the tilt angle orientation of water molecules. Our results, obtained with first-principles methods, strongly support the need to account for polarizability when describing aqueous salt solutions near a hydrophobic interface and provide important predictions for comparison to future experimental measurements.

AUTHOR INFORMATION

Corresponding Author

*E-mail: gagalli@ucdavis.edu.

Notes

The authors declare no competing financial interest.

ACKNOWLEDGMENTS

This work was partly performed under the auspices of the U.S. Department of Energy by the Lawrence Livermore National Laboratory under Contract No. DE-AC52-07NA27344 and was supported by the DOE/CMCSN Structure and Dynamics of Water and Aqueous Solutions Collaborative Research Team. H.J.K. holds a Career Award at the Scientific Interface from the Burroughs Wellcome Fund.

REFERENCES

(1) Rasaiah, J. C.; Garde, S.; Hummer, G. Water in Nonpolar Confinement: From Nanotubes to Proteins and Beyond. *Annu. Rev. Phys. Chem.* **2008**, *59*, 713−740.

(2) Bryant, R. The Dynamics of Water−Protein Interactions. *Annu. Rev. Biophys. Biom.* **1996**, *25*, 29−53.

(3) Israelachvili, J.; Wennerstrom, H. Role of Hydration and Water Structure in Biological and Colloidal Interactions. *Nature* **1996**, *379*, 219−225.

(4) Balavoine, F.; Schultz, P.; Richard, C.; Mallouh, V.; Ebbesen, T.; Mioskowski, C. Helical Crystallization of Proteins on Carbon Nanotubes: A First Step Towards the Development of New Biosensors. *Angew. Chem., Int. Ed.* **1999**, *38*, 1912−1915.

(5) Nguyen, C.; Delzeit, L.; Cassell, A.; Li, J.; Han, J.; Meyyappan, M. Preparation of Nucleic Acid Functionalized Carbon Nanotube Arrays. *Nano Lett.* **2002**, *2*, 1079−1081.

(6) Holt, J.; Park, H.; Wang, Y.; Stadermann, M.; Artyukhin, A.; Grigoropoulos, C.; Noy, A.; Bakajin, O. Fast Mass Transport through Sub-2-nanometer Carbon Nanotubes. *Science* **2006**, *312*, 1034−1037.

(7) Majumder, M.; Chopra, N.; Andrews, R.; Hinds, B. Nanoscale Hydrodynamics — Enhanced Flow in Carbon Nanotubes. *Nature* **2005**, *438*, 44−44.

(8) Karaborni, S.; Smit, B.; Heidug, W.; Urai, J.; vanOort, E. The Swelling of Clays: Molecular Simulations of the Hydration of Montmorillonite. *Science* **1996**, *271*, 1102−1104.

(9) Levi, M. D.; Sigalov, S.; Salitra, G.; Elazari, R.; Aurbach, D. Assessing the Solvation Numbers of Electrolytic Ions Confined in Carbon Nanopores under Dynamic Charging Conditions. *J. Phys. Chem. Lett.* **2011**, *2*, 120−124.

(10) Cicero, G.; Grossman, J. C.; Schwegler, E.; Gygi, F.; Galli, G. Water Confined in Nanotubes and Between Graphene Sheets: A First Principle Study. *J. Am. Chem. Soc.* **2008**, *130*, 1871−1878.

(11) Donadio, D.; Cicero, G.; Schwegler, E.; Sharma, M.; Galli, G. Electronic Effects in the IR Spectrum of Water Under Confinement. *J. Phys. Chem. B* **2009**, *113*, 4170−4175.

(12) Huang, P.; Schwegler, E.; Galli, G. Water Confined in Carbon Nanotubes: Magnetic Response and Proton Chemical Shieldings. *J. Phys. Chem. C* **2009**, *113*, 8696−8700.

(13) Sharma, M.; Donadio, D.; Schwegler, E.; Galli, G. Probing Properties of Water under Confinement: Infrared Spectra. *Nano Lett.* **2008**, *8*, 2959−2962.

(14) Naguib, N.; Ye, H.; Gogotsi, Y.; Yazicioglu, A. G.; Megaridis, C. M.; Yoshimura, M. Observation of Water Confined in Nanometer Channels of Closed Carbon Nanotubes. *Nano Lett.* **2004**, *4*, 2237−2243.

(15) Fornasiero, F.; Park, H. G.; Holt, J. K.; Stadermann, M.; Grigoropoulos, C. P.; Noy, A.; Bakajin, O. Ion Exclusion by Sub-2-nm Carbon Nanotube Pores. *Proc. Natl. Acad. Sci. U.S.A.* **2008**, *105*, 17250−17255.

(16) Caminiti, R.; Licheri, G.; Piccaluga, G.; Pinna, G. X-ray-Diffraction Study of a 3-Ion Aqueous-Solution. *Chem. Phys. Lett.* **1977**, *47*, 275−278.

(17) Probst, M.; Radnai, T.; Heinzinger, K.; Bopp, P.; Rode, B. Molecular-Dynamics and X-ray Investigation of an Aqueous $CaCl_2$ Solution. *J. Phys. Chem.* **1985**, *89*, 753−759.

(18) Skipper, N.; Neilson, G. X-ray and Neutron-Diffraction Studies on Concentrated Aqueous-Solutions of Sodium-Nitrate and Silver-Nitrate. *J. Phys.: Condens. Matter* **1989**, *1*, 4141−4154.

(19) Fulton, J. L.; Heald, S. M.; Badyal, Y. S.; Simonson, J. M. Understanding the Effects of Concentration on the Solvation Structure of Ca^{2+} in Aqueous Solution. I: The Perspective on Local Structure from EXAFS and XANES. *J. Phys. Chem. A* **2003**, *107*, 4688−4696.

(20) Enderby, J. E. Ion Solvation via Neutron-Scattering. *Chem. Soc. Rev.* **1995**, *24*, 159−168.

(21) Hewish, N. A.; Neilson, G. W.; Enderby, J. E. Environment of Ca^{2+} Ions in Aqueous Solvent. *Nature* **1982**, *297*, 138−139.

(22) Cappa, C. D.; Smith, J. D.; Messer, B. M.; Cohen, R. C.; Saykally, R. J. Effects of Cations on the Hydrogen Bond Network of Liquid Water: New Results from X-ray Absorption Spectroscopy of Liquid Microjets. *J. Phys. Chem. B* **2006**, *110*, 5301−5309.

(23) Bruni, F.; Imberti, S.; Mancinelli, R.; Ricci, M. A. Aqueous Solutions of Divalent Chlorides: Ions Hydration Shell and Water Structure. *J. Chem. Phys.* **2012**, *136*, 064520.

(24) Tongraar, A.; Liedl, K. R.; Rode, B. M. Solvation of Ca^{2+} in Water Studied by Born-Oppenheimer Ab Initio QM/MM Dynamics. *J. Phys. Chem. A* **1997**, *101*, 6299−6309.
(25) Alexiadis, A.; Kassinos, S. Molecular Simulation of Water in Carbon Nanotubes. *Chem. Rev.* **2008**, *108*, 5014−5034.
(26) Kumar, P.; Buldyrev, S. V.; Starr, F. W.; Giovambattista, N.; Stanley, H. E. Thermodynamics, Structure, and Dynamics ofWater Confined between Hydrophobic Plates. *Phys. Rev. E* **2005**, *72*, 051503.
(27) Choudhury, N.; Pettitt, B. M. Dynamics of Water Trapped between Hydrophobic Solutes. *J. Phys. Chem. B* **2005**, *109*, 6422−6429.
(28) Kalra, A.; Garde, S.; Hummer, G. Osmotic Water Transport Through Carbon Nanotube Membranes. *Proc. Natl. Acad. Sci. U.S.A.* **2003**, *100*, 10175−10180.
(29) Mashl, R. J.; Joseph, S.; Aluru, N. R.; Jakobsson, E. Anomalously Immobilized Water: A New Water Phase Induced by Confinement in Nanotubes Phase Induced by Confinement in Nanotubes. *Nano Lett.* **2003**, *3*, 589−592.
(30) Werder, T.; Walther, J. H.; Jaffe, R. L.; Halicioglu, T.; Koumoutsakos, P. On the Water−Carbon Interaction for Use in Molecular Dynamics Simulations of Graphite and Carbon Nanotubes. *J. Phys. Chem. B* **2003**, *107*, 1345−1352.
(31) Xu, S.; Irle, S.; Musaev, D. G.; Lin, M. C. Water Clusters on Graphite: Methodology for Quantum Chemical A Priori Prediction of Reaction Rate Constants. *J. Phys. Chem. A* **2005**, *109*, 9563−9572.
(32) White, J. A.; Schwegler, E.; Galli, G.; Gygi, F. The Solvation of Na^{+} in Water: First-Principles Simulations. *J. Chem. Phys.* **2000**, *113*, 4668−4673.
(33) Kulik, H. J.; Marzari, N.; Correa, A. A.; Prendergast, D.; Schwegler, E.; Galli, G. Local Effects in the X-ray Absorption Spectrum of Salt Water. *J. Phys. Chem. B* **2010**, *114*, 9594−9601.
(34) Jungwirth, P.; Tobias, D. Specific Ion Effects at the Air/Water Interface. *Chem. Rev.* **2006**, *106*, 1259−1281.
(35) Perdew, J. P.; Burke, K.; Ernzerhof, M. Generalized Gradient Approximation Made Simple. *Phys. Rev. Lett.* **1996**, *77*, 3865−3868.
(36) *QBOX*, A Large-Scale Parallel Implementation of First-Principles Molecular Dynamics. http://eslab.ucdavis.edu (2012).
(37) Schwegler, E.; Grossman, J.; Gygi, F.; Galli, G. Towards an Assessment of the Accuracy of Density Functional Theory for First Principles Simulations of Water. II. *J. Chem. Phys.* **2004**, *121*, 5400−5409.
(38) Giannozzi, P.; Baroni, S.; Bonini, N.; Calandra, M.; Car, R.; Cavazzoni, C.; Ceresoli, D.; Chiarotti, G. L.; Cococcioni, M.; Dabo, I.; et al. QUANTUM ESPRESSO: A Modular and Open-Source Software Project for Quantum Simulations of Materials. *J. Phys.: Condens. Matter* **2009**, *21*, 395502.
(39) Prendergast, D.; Galli, G. X-ray Absorption Spectra of Water from First Principles Calculations. *Phys. Rev. Lett.* **2006**, *96*, 215502.
(40) Hetenyi, B.; De Angelis, F.; Giannozzi, P.; Car, R. Calculation of Near-Edge X-ray-Absorption Fine Structure at Finite Temperatures: Spectral Signatures of Hydrogen Bond Breaking in Liquid Water. *J. Chem. Phys.* **2004**, *120*, 8632−8637.
(41) Taillefumier, M.; Cabaret, D.; Flank, A.-M.; Mauri, F. X-ray Absorption Near-Edge Structure Calculations with the Pseudopotentials: Application to the K Edge in Diamond and Alphaquartz. *Phys. Rev. B* **2002**, *66*, 195107.
(42) Blöchl, P. E. Projector Augmented-Wave Method. *Phys. Rev. B* **1994**, *50*, 17953−17979.
(43) Schwartz, C. P.; Uejio, J. S.; Saykally, R. J.; Prendergast, D. On the Importance of Nuclear Quantum Motions in Near Edge X-ray Absorption Fine Structure Spectroscopy of Molecules. *J. Chem. Phys.* **2009**, 130.
(44) Brown, E. C.; Mucha, M.; Jungwirth, P.; Tobias, D. J. Structure and Vibrational Spectroscopy of Salt Water/Air Interfaces: Predictions from Classical Molecular Dynamics Simulations. *J. Phys. Chem. B* **2005**, *109*, 7934−7940.
(45) D'Auria, R.; Tobias, D. J. Relation Between Surface Tension and Ion Adsorption at the Air−Water Interface: A Molecular Dynamics Simulation Study. *J. Phys. Chem. A* **2009**, *113*, 7286−7293.
(46) Sala, J.; Guardia, E.; Marti, J. Specific Ion Effects in Aqueous Eletrolyte Solutions Confined within Graphene Sheets at the Nanometric Scale. *Phys. Chem. Chem. Phys.* **2012**, *14*, 10799−10808.
(47) Callahan, K. M.; Casillas-Ituarte, N. N.; Xu, M.; Roeselová, M.; Allen, H. C.; Tobias, D. J. Effect of Magnesium Cation on the Interfacial Properties of Aqueous Salt Solutions. *J. Phys. Chem. A* **2010**, *114*, 8359−8368.
(48) Baer, M. D.; Mundy, C. J. Toward an Understanding of the Specific Ion Effect Using Density Functional Theory. *J. Phys. Chem. Lett.* **2011**, *2*, 1088−1093.
(49) dos Santos, A. P.; Levin, Y. Ion Specificity and the Theory of Stability of Colloidal Suspensions. *Phys. Rev. Lett.* **2011**, *106*, 167801.
(50) Calero, C.; Faraudo, J.; Bastos-Gonzalez, D. Interaction of Monovalent Ions with Hydrophobic and Hydrophilic Colloids: Charge Inversion and Ionic Specificity. *J. Am. Chem. Soc.* **2011**, *133*, 15025−15035.
(51) Kunz, W. Specific Ion Effects in Colloidal and Biological Systems. *Curr. Opin. Colloid Interface Sci.* **2010**, *15*, 34−39.
(52) Caleman, C.; Hub, J. S.; van Maaren, P. J.; van der Spoel, D. Atomistic Simulation of Ion Solvation in Water Explains Surface Preference of Halides. *Proc. Natl. Acad. Sci. U.S.A.* **2011**, *108*, 6838−6842.
(53) Petersen, P. B.; Saykally, R. J. On the Nature of Ions at the Liquid Water Surface. *Annu. Rev. Phys. Chem.* **2006**, *57*, 333−364.